Proc. Natl. Acad. Sci. USA
Vol. 87, pp. 3552–3556, May 1990
Biophysics

Evidence that a distribution of bacterial reaction centers underlies the temperature and detection-wavelength dependence of the rates of the primary electron-transfer reactions

CHRISTINE KIRMAIER AND DEWEY HOLTEN

Department of Chemistry, Washington University, Saint Louis, MO 63130

Communicated by George Feher, February 20, 1990 (received for review December 8, 1989)

ABSTRACT **The rates of the primary electron-transfer processes in *Rhodobacter sphaeroides* reaction centers have been examined in detail by using 150-fs excitation flashes at 870 nm. At room temperature the apparent time constants for both initial charge separation ($P^* \rightarrow P^+BPh_L^-$) and subsequent electron transfer ($P^+BPh_L^- \rightarrow P^+Q_A^-$) are found to encompass a range of values (≈1.3–4 ps and ≈100–320 ps, respectively), depending on the wavelength at which the kinetics are followed. We suggest this reflects a distribution of reaction centers (or a few conformers), having differences in factors such as distances or orientations between the cofactors, hydrogen bonding, or other pigment–protein interactions. We also suggest that the time constants observed at cryogenic temperatures (≈1.3 and ≈100 ps, respectively, with much smaller or negligible variation with detection wavelength) do not reflect an actual increase in the rates with decreasing temperature but rather derive from a shift in the distribution of reaction centers toward those in which electron transfer inherently occurs with the faster rates.**

The temperature dependence of the rates of electron transfer in bacterial reaction centers (RCs) has received considerable experimental and theoretical attention. The rate of recombination between the oxidized dimer of bacteriochlorophyll (BChl) molecules, P, and the reduced quinone acceptor, Q_A^-, ($P^+Q_A^- \rightarrow PQ_A$) was the first to be investigated as a function of temperature followed, as technology advanced, by the rate of electron transfer from the bacteriopheophytin (BPh) anion to Q_A ($P^+BPh_L^- \rightarrow P^+Q_A^-$) and by the recent investigations of initial charge separation, $P^* \rightarrow P^+BPh_L^-$. [The L and M subscripts refer to the polypeptide to which a particular component is either bound or most closely associated (1–3).] All three reactions are characterized by at least a 2-fold increase in observed rate constant between room and cryogenic temperatures (see refs. 4–10 and citations therein).

For the most part the temperature dependence of the initial charge separation step (observed to occur in ≈3 ps at 295 K and ≈1 ps at 10 K) has been followed via the decay of the broad stimulated emission band of P*, which has a maximum near 920 nm in *Rhodobacter sphaeroides* (6, 7). The temperature dependence of electron transfer from BPh_L^- to Q_A in *Rb. sphaeroides* ($\tau \approx 200$ ps at 295 K and ≈ 100 ps at 77 K and below) similarly has been followed primarily in a single region, namely via decay of the broad BPh_L anion band centered near 665 nm (5). Kinetics also have been measured at a few wavelengths near 800 nm in the recent studies of the $P^* \rightarrow P^+BPh_L^-$ process, with the primary focus being a search for evidence for the possible transient reduction of the monomeric pigment $BChl_L$ (6, 7, 11, 12). During the course of our previous investigations of electron transfer from BPh_L^- to Q_A, we examined the near-infrared (730–830 nm) region also, with the expectation of finding time constants that agreed with those measured via decay of the BPh_L anion band. This proved not to be uniformly the case, however. At room temperature, for example, we found that at certain wavelengths the observed time constant was somewhat less than 200 ps, and at other wavelengths it was somewhat greater than 200 ps (5). A major limitation of these measurements was that the signal-to-noise ratio prevented a complete study in the near-infrared region in that accurate time constants at room temperature could be measured only within two narrow (≈5 nm) wavelength regions centered near the peak ground state absorptions of the BPhs and the monomeric BChls.

We have reexamined these findings by using instrumentation that gives a significantly better signal-to-noise ratio in ΔA and, in addition, utilizes 150-fs flashes (compared to the 30-ps flashes used in the older studies). The shorter flashes allow us to investigate the initial electron transfer step(s) as well. We show here that the overall conversion of P* to $P^+Q_A^-$ is manifest in the 80-nm interval spanning the Q_Y absorption bands of the chromophores (740–820 nm) as an intricate detection wavelength dependence of the apparent rates for both electron transfer processes. A physically reasonable model for these results is presented.

MATERIALS AND METHODS

Isolation of *Rb. sphaeroides* R26 RCs followed published procedures (4). For the room temperature measurements, 10–15 μM RCs in 10 mM Tris buffer, pH 7.8/0.05% lauryl dimethylamine-*N*-oxide (LDAO) were flowed through a 2-mm-path-length cell while being maintained at 285 K. The measurements at 77 K used RCs embedded in poly(vinyl alcohol) (PVA) films (having $A_{800} \approx 0.6$–1) and an Oxford Instruments cryostat. Transient absorption spectra and kinetics were measured on a spectrometer that utilizes 150-fs flashes and gives a standard deviation in ΔA of ±0.005 (12). The 15-μJ 870-nm excitation flashes were polarized at 45° with respect to white-light probe pulses to minimize dichroism of the absorption changes. The excitation flashes were focused to ≈0.5–1 mm at the sample and typically excited 20–25% of the RCs.

RESULTS AND DISCUSSION

Electron-Transfer Kinetics. Fig. 1 shows 285 K transient absorption difference spectra between 720 and 840 nm observed 330 fs, 11.4 ps, and 2.7 ns after excitation. The spectra at these times can be assigned to P*, $P^+BPh_L^-$, and $P^+Q_A^-$, respectively, and the time evolution of the spectra reflects the electron-transfer processes $P^* \rightarrow P^+BPh_L^-$ and $P^+BPh_L^- \rightarrow P^+Q_A^-$. To analyze the rates of these two processes, the absorption changes spanning ≈300 fs to ≈3 ns were averaged

The publication costs of this article were defrayed in part by page charge payment. This article must therefore be hereby marked "*advertisement*" in accordance with 18 U.S.C. §1734 solely to indicate this fact.

Abbreviations: RC, reaction center; BChl, bacteriochlorophyll; BPh, bacteriopheophytin; P, a BChl dimer; Q_A, primary quinone.

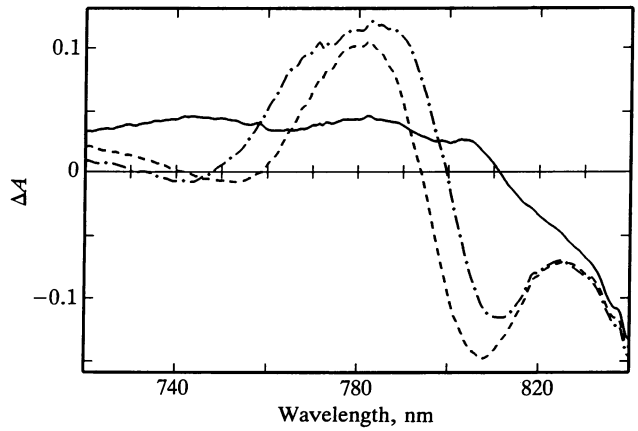

FIG. 1. Transient absorption spectra at 285 K acquired 330 fs (——), 11.4 ps (------), and 2.7 ns (−·−) following excitation of 15 μM *Rb. sphaeroides* R26 RCs with 150-fs 870-nm flashes.

over 3-nm intervals and fit to a constant plus two exponentials [$\Delta A = \Delta A_\infty + B \exp(-t/\tau_1) + C \exp(-t/\tau_2)$, where τ_1 is the time constant for $P^* \rightarrow P^+BPh_L^-$ electron transfer, τ_2 is the time constant for electron transfer from BPh_L^- to Q_A and t is the time after excitation]. (The averaged intervals were 720–722, 723–725, . . . 828–830, and the results for these intervals will be referred to as the time constants measured at 721 nm, 724 nm, etc.) When the total change in ΔA with time was less than 4 standard deviations in ΔA (i.e., less than 0.02), the resulting value of τ_1 or τ_2, or both as the case may be, was not incorporated into the final results. This was true, for example, for τ_2 from ≈770 to ≈780 nm in all experiments at both 285 and 77 K. We adopt this two-step model to begin this close examination of the near-infrared data. The controversial possibility that the monomeric $BChl_L$ acts as an intermediate electron carrier between P* and BPh_L^- will be addressed further below.

Fig. 2 shows a plot of the wavelength dependence of the time constants derived from the dual exponential fits of the 285 K data (solid symbols). It can be seen that there are two regions within which there is about a 3-fold variation in both τ_1 and τ_2. Between 787 and 815 nm and between 770 and 750 nm, τ_2 varies from ≈100 ps to ≈300 ps, changing by ≈10 ps/nm. The average value of τ_2 in both regions is ≈200 ps. A

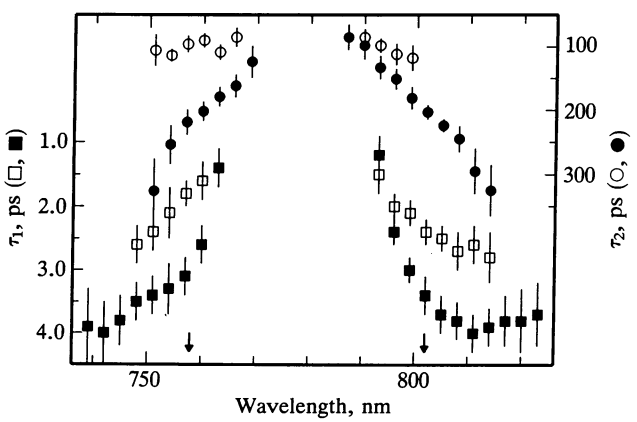

FIG. 2. Wavelength variance of the time constants from the dual exponential fits of the near-infrared absorption changes in *Rb. sphaeroides* R26 RCs at 285 K (closed symbols) and 77 K (open symbols). τ_1 (squares) and τ_2 (circles) are the fit time constants for $P^* \rightarrow P^+BPh_L^-$ and $P^+BPh_L^- \rightarrow P^+Q_A^-$ electron transfer, respectively. The observation that the apparent time constant for both electron-transfer reactions is wavelength dependent is a manifestation of the distribution model developed in the text. (The arrows on the abscissa mark the peak positions of the ground state Q_Y absorption bands.)

similar but not identical pattern is observed for τ_1, which varies from ≈1.3 ps at 793 and 763 nm to almost 4 ps at wavelengths ≥810 and ≤745 nm. Note that the two regions over which the observed time constants vary are roughly centered on the maxima of the ground state Q_Y absorption bands of the monomeric BChls (802 nm) and BPhs (758 nm).

The data at 796 and 805 nm and the associated fits shown in Fig. 3 are an example of typical results from one measurement. The full data sets (spanning 300 fs to 3 ns) and dual exponential fits are shown in Fig. 3*A Inset* and Fig. 3*B Inset*. Fig. 3 compares portions of the data, 0–10 ps (Fig. 3*A*) and 0–1 ns (Fig. 3*B*), with the ordinates chosen so that the data for both wavelengths span the same full-scale vertical displacement. (This facilitates direct visual comparison of the data and fits.) The dual exponential fits shown give τ_1 = 2.4 ± 0.2 ps and τ_2 = 163 ± 9 ps at 796 nm, and τ_1 = 3.7 ± 0.2 ps and τ_2 = 258 ± 23 ps at 805 nm. Fig. 3 shows that even though the two values of τ_1 at these wavelengths differ by only about one-half the overall span of values obtained, the data are clearly well resolved from one another. The same obviously is true for the pair of τ_2 values as well.

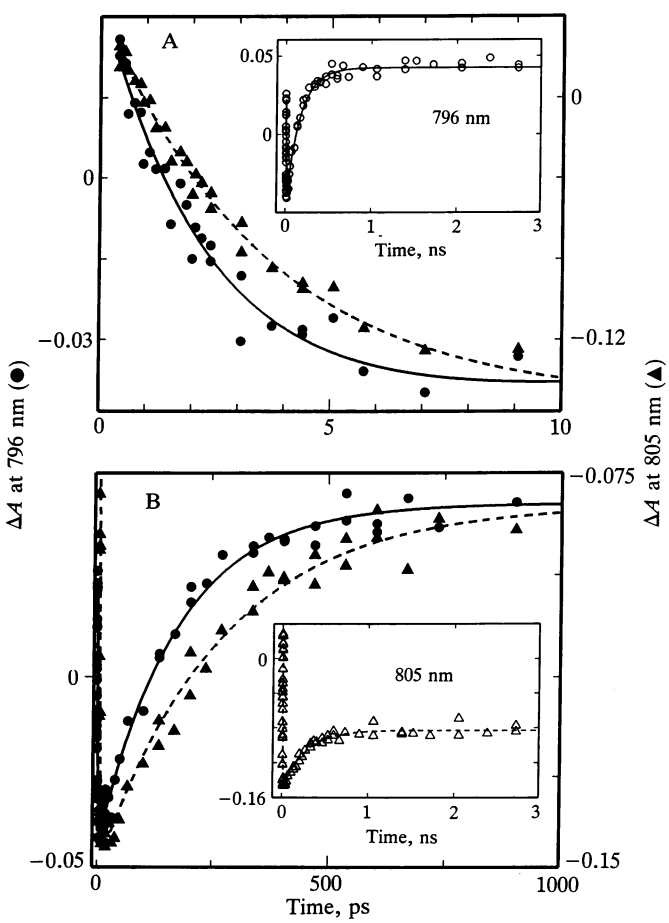

FIG. 3. Kinetic data at 796 nm (circles) and 805 nm (triangles) from a typical measurement displayed on the timescales of 0–10 ps (*A*) and 0–1 ns (*B*). The complete data sets (spanning 300 fs to 3 ns) are shown in the insets. The solid line in *A*, *B*, and *A Inset* is a dual exponential fit of the 796-nm data, giving apparent time constants of 2.4 ± 0.2 ps and 163 ± 9 ps for electron transfer from P* to BPh_L, and from BPh_L^- to Q_A, respectively. The dashed line in *A*, *B*, and *B Inset* is a dual exponential fit of the 805-nm data, giving apparent time constants of 3.7 ± 0.2 ps and 258 ± 23 ps for these two processes. (Open symbols have been used in *Insets* so as to clearly distinguish the individual points. The differences between the ordinate scales in the three displays of the data at a given wavelength result from the three different timescales over which the data and fits are compared.)

Measurements were also performed on RCs in poly(vinyl alcohol) films at 77 K, and the data analyzed via the same procedures as were applied to the 285 K data. The results are given by the open symbols in Fig. 2. The narrowing and sharpening of the spectral features at 77 K compared with 285 K reduces the widths of the spectral regions over which the electron-transfer kinetics can be followed. It can be seen, however, that at 77 K, the wavelength variation of the rate for BPh_L^- to Q_A electron transfer is essentially absent; τ_2 is constant at ≈100 ps over regions where it varies by more than a factor of 2 at 285 K. A detection-wavelength dependence of the apparent $P^* \rightarrow P^+BPh_L^-$ electron-transfer rate still remains at 77 K, but the range of τ_1 values (≈1.3 to ≈2.6 ps) is reduced by ≈50% from that found at 285 K.

Distribution Model. In an earlier study on *Rb. sphaeroides* RCs utilizing 30-ps flashes at 600 nm, we reported that although a time constant of ≈200 ps was measured for electron transfer from BPh_L^- to Q_A at 285 K via decay of the BPh_L anion band near 665 nm, somewhat longer and shorter time constants were measured near 765 and 795 nm, respectively (5). While not a completely satisfactory explanation, we offered the suggestion that the different kinetics in the near infrared might reflect readjustments of the chromophores and/or the protein in response to electron transfer. We considered this same possibility in a more recent study on *Rb. capsulatus* RCs upon finding that the time constant measured near 785 nm appeared to be somewhat longer than the ≈3 ps observed at 800 nm and for the decay of P* stimulated emission (12).

The present work vastly extends these results to include a full characterization of the detection-wavelength dependence of the time constant not only for BPh_L^- to Q_A electron transfer but also for initial charge separation. A key finding here is that at 285 K the shortest time constants observed for both processes, ≈1.3 and ≈100 ps, are essentially identical to those previously measured only at cryogenic temperatures (5, 7). This fact and the strikingly similar patterns seen in Fig. 2 for the apparent time constants for both reactions suggest a common origin for the results other than the pigment–protein relaxations described above. We propose this to be a distribution of RCs (or perhaps just a small number of conformers) encompassing roughly a 3-fold variation of the rates of electron transfer at room temperature. Some fraction of the RCs carry out electron transfer with the faster rates, $\approx(1.3\text{ ps})^{-1}$ and $\approx(100\text{ ps})^{-1}$; some, with the comparatively slower rates $\approx(4\text{ ps})^{-1}$ and $\approx(300\text{ ps})^{-1}$; and others, likely the majority at 285 K, with intermediate rates. The data in Fig. 2 further show that mean rates (≈3 ps and ≈200 ps) are observed near the peaks of the ground state absorption maxima (760 and 800 nm). The different RCs in the distribution apparently interconvert on a timescale longer than that of the primary photochemistry (i.e., >1 ns), leading to an inhomogeneous population that gives rise to the variation in the observed time constants as a function of detection wavelength. Hence, the values of the time constants reflect the weighted contributions of the members of the distribution at any given probe wavelength. We further suggest that at low temperatures the RCs become frozen into the "fast" form, or at least a much smaller distribution weighted toward the faster forms.

It is important to note that the apparent span of rates for both electron-transfer processes is only a factor of 3; hence, the differences among the members of the population probed at any one wavelength are likely to be even smaller. Such differences are sufficiently small that good exponential fits are obtained at most wavelengths. However, an exception to this is the data between about 770 and 790 nm, where an exponential for $P^* \rightarrow P^+BPh_L^-$ (τ_1) and an exponential for $P^+BPh_L^- \rightarrow P^+Q_A^-$ (τ_2) do not fit the data nearly as well as at other wavelengths. At some wavelengths in this region, somewhat better fits could be obtained with three exponentials as shown in Fig. 4. It is particularly noteworthy that the time constants returned from these fits include a pair of short or long values (e.g., ≈1, ≈3, and ≈100 ps or ≈4, ≈100, and ≈300 ps), which are within the range of values found at other wavelengths. It is also noteworthy that a given pair of close-valued time constants corresponds to absorption changes in opposite directions (the preexponential factors have opposite signs). This makes it easier to resolve significant deviation from single-exponential behavior even though the differences in the time constants (on both timescales) are still a factor of three or less.

Particularly complex overlapping absorption changes and kinetics between 770 and 790 nm can be expected, especially in the presence of a distribution of RCs, since this region of the transient spectra is the most congested. At a minimum it is comprised of (*i*) the appearance of new absorption due to the blue- and red-shifts of the Q_Y bands of the monomeric BChls and the BPhs, respectively, in response to P^+ (and possibly P*) formation; (*ii*) additional and time-dependent electrochromic shifts in response to BPh_L^- formation and decay; and (*iii*) the bleaching and recovery of the Q_Y band of BPh_L. The finding of ≈1- and ≈3-ps time constants at 785 nm in ref. 13 is consistent with the results reported here; however, in ref. 13 the results were assigned to the transient formation (3 ps) and decay (1 ps) of $P^+BChl_L^-$. Clearly $P^+BChl_L^-$ cannot be invoked to explain the finding of the strikingly similar detection-wavelength-dependent kinetics on the 100- to 300-ps timescale of the $P^+BPh_L^- \rightarrow P^+Q_A^-$ process (Fig. 2). Since the alternative model of a distribution of RC conformers provides a consistent and physically reasonable explanation for the complex kinetic patterns on both timescales, the $P^* \rightarrow P^+BChl_L^- \rightarrow P^+BPh_L^-$ model of charge separation remains experimentally unproven (see also refs. 6, 7, 11, 12, and 14).

The present level of data analysis provides no quantitative information on the details of the proposed distribution. Arriving at such information will, indeed, be a nontrivial task and model dependent. For example, one could try fitting the data to the sum of many exponentials for both $P^* \rightarrow P^+BPh_L^-$ and $P^+BPh_L^- \rightarrow P^+Q_A^-$ electron transfer, or the sum of two stretched exponentials, or to the sum of two polynomial functions (e.g., see refs. 4 and 15). Even the next most simple step beyond the current analysis—namely, fitting the kinetic data wavelength by wavelength to a sum of four exponentials (two for $P^* \rightarrow P^+BPh_L^-$ and two for $P^+BPh_L^- \rightarrow P^+Q_A^-$)—will

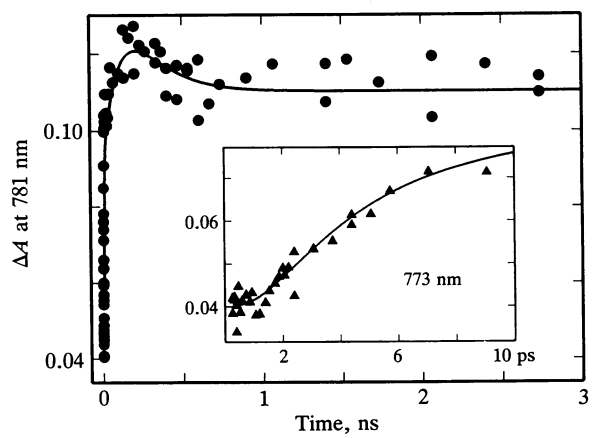

FIG. 4. Three exponential fits to the absorption changes at 781 nm and 773 nm (*Inset*), giving time constants of 4.3 ± 1.6, 107 ± 150, and 226 ± 270 ps (781 nm) and 1.1 ± 1.7, 3.5 ± 2.4, and 65 ± 18 ps (773 nm). Although the errors are large (see text), the trends in the values of the time constants are consistent with the distribution model.

not yield direct information on even the fractional contributions of fast/slow components as a function of wavelength, because numerous assumptions about extinction coefficients and electrochromic band shifts associated with each transient state and each member of the distribution would have to be made. We believe a more restrictive and informative approach will be to perform a global simulation of the time evolution of the transient absorption spectra spanning 300 fs to 3 ns and 500 to 1000 nm as a function of temperature. The observation that we have reported here—that the apparent time constants resulting from simple single-exponential fits to *both* individual electron-transfer reactions vary with wavelength—already clearly exposes the underlying physical model—namely, that we are not dealing with a simple homogeneous population of RCs but rather with an inhomogeneous distribution of RCs with slightly differing spectral and kinetic properties, particularly at room temperature.

Relationships to Other Work. Our distribution model relates to a number of other issues and previous experimental results as well. Perhaps foremost is the generally held belief that the rates of electron transfer increase with decreasing temperature, although this has always been tempered with the caveat that the observed increases at low temperature could be due, at least in part, to contraction of the protein (e.g., see refs. 4–10 and 16–18). Our results suggest that the time constants measured at low temperatures may not reflect an actual increase in the rates of electron transfer but rather stem from a shifting of a distribution of RCs to favor those in which electron transfer inherently occurs with faster rates. This represents a departure from the previous interpretation, although the underlying conceptual framework of electron transfer in the RC—that it is basically activationless—remains intact. Much less demanding constraints on the relationship between the free-energy change and reorganization energy are required for a process that is independent of temperature as opposed to a reaction that increases in rate as the temperature is reduced.

We suggest that the values of time constants for the primary electron-transfer reactions obtained in the majority of previous studies actually reflect the average time constants for the distribution, since most measurements have monitored the rate of initial charge separation via decay of the P* stimulated emission band and of electron transfer from BPh_L^- to Q_A via the decay of the BPh_L anion. Both of these are inherently broad (≈100 nm) features—i.e., their widths are not derived primarily from the distribution of RC types that we are proposing, although this may contribute to some extent. Hence, we suggest that all RCs in the distribution contribute more or less equally across these broad features, and it is for this reason that we propose that one basically measures a mean time constant in these regions. In keeping with this, we have found that 200 ± 20 ps is obtained at 285 K throughout 640–690 nm (covering most of the BPh_L anion band) for electron transfer from BPh_L^- to Q_A (5), in contrast to the 100- to 300-ps range of values reported here in the near infrared over much smaller wavelength intervals. Note that the 200-ps time constant measured in the anion band equals the midpoint of the Q_Y range at 285 K. Similarly, we have measured a time constant at 285 K of 3.3 ± 0.3 ps through the main part of the stimulated emission band (900–940 nm), using either 582- or 870-nm excitation flashes (data not shown). Again, this value is in between the extremes of 1.3 and 4 ps measured in the Q_Y band region (Fig. 2) but, interestingly, is weighted slightly toward the longer values of τ_1.

These parallels between the average time constants derived from the anion and stimulated emission bands and the Q_Y region variations in τ_1 and τ_2 also hold at low temperature. Our previous observation that the (distribution average) value of τ_2 measured in the BPh_L anion band decreases roughly by a factor of 2 between 285 and 100 K and then remains constant at ≈100 ps down to 5 K (5) parallels the observation that the Q_Y region detection-wavelength dependence of τ_2 is essentially absent at 77 K, the distribution having collapsed toward the members with the shortest (≈100 ps) time constants (Fig. 2). For electron transfer from P* to BPh_L, the (distribution average) value of τ_1 measured via P* stimulated emission decay continues to change below 77 K, having values at 295, 77, and 10 K of 2.8, 1.6, and 1.2 ps, respectively (7). [Our values, 3.3, 1.8, and 1.4 ps at 285, 77, and 5 K, respectively (data not shown), are in good agreement with these previous measurements.] Again the parallel holds in that a distribution of τ_1 values in the Q_Y region remains at 77 K, although it is much smaller than at room temperature. Since the (distribution average) time constant of ≈1.3 ps for decay of stimulated emission at liquid helium temperatures is the same as the smallest τ_1 value obtained at 285 and 77 K (Fig. 2), our model suggests that a roughly Q_Y wavelength-invariant time constant of ≈1.3 ps will be found at 5 K for the initial electron transfer reaction. A further parallel exists between the average value and distribution width of the time constant for initial charge separation and the position and width of the ground state absorption band of P (16, 18)—namely, all of these observables continue to change below 100 K.

The simple qualitative parallels seen in Fig. 2 for the wavelength and temperature variations of τ_1 and τ_2 may stem from molecular factors involving BPh_L, since both $P^* \rightarrow P^+BPh_L^-$ and $P^+BPh_L^- \rightarrow P^+Q_A^-$ processes involve this molecule. Differences in the degree of hydrogen bonding between the C-10 keto group of BPh_L and the adjacent glutamic acid residue (Glu^{L104}) are known to affect the rates of both electron transfer from P* to BPh_L and from BPh_L^- to Q_A. Replacement of Glu^{L104} in *Rb. capsulatus* with leucine or glutamine increases the (distribution average) time constants of both reactions from 3.5 and 200 ps in wild-type to 5.5 and 270 ps in the mutants (19). Such an effect on the rate of the initial electron-transfer reaction was predicted by theory (20). In *C. aurantiacus*, where the analogous residue is glutamine, the mean time constants for both reactions (8 and 320 ps) are also both longer than in wild-type RCs from other organisms (21, 22). Recent resonance Raman measurements have indicated that the Bph_L–Glu^{L104} hydrogen-bonding interaction and the planarity of the BPh_L macrocycle may be temperature dependent (29), providing a potential connection with the temperature dependence of the distribution of rates. Molecular factors involving P may provide additional variables giving rise to the detailed differences between the patterns in τ_1 and τ_2 discussed above. This relates back to the observation that the ground state spectrum of P changes with temperature in a manner similar to how the average value and distribution width of the rate of $P^* \rightarrow P^+BPh_L^-$ change. A possibility for such a factor is the interring separation between the two BChls of P (16–18).

The fact that the variations in τ_1 and τ_2 with wavelength are monotonic in Fig. 2 points to a limited set of molecular factors underlying the distribution. We have detailed a few possibilities above. This is opposed to a more complicated or even random pattern that might emerge if many different, perhaps unrelated, factors were important. Our results are consistent with a potential energy surface containing barriers between different substates of the distribution, making their interconversion slower (>1 ns) than the primary electron-transfer reactions. These barriers may reflect restricted pigment/protein motions involving hydrogen bonds, porphyrin ring puckering/flattening, or torsional motions of various types. Lowering the temperature apparently results in the collapse of the room-temperature distribution of RCs toward a form (or small number of substates) with the fastest rates. A major contribution to this may be a general contraction of the

protein at low temperature. In this regard the average interatomic distance in myoglobin decreases by 3% between 295 and 77 K (23). If different interchromophore or pigment–protein distances partly (or completely) underly the distribution, then one can readily understand why lowering the temperature results in a collapse to the RC form(s) with the fastest inherent rates of electron transfer. This provides a global means in addition to (or instead of) specific molecular interactions for understanding the temperature behavior of the distribution.

The results presented here can be compared with previous studies of other RC properties. Recent studies on *Rhodopseudomonas viridis* RCs have found biphasic $P^+Q_A^-$ (and $P^+Q_B^-$) charge recombination kinetics at 295 K with the relative amplitudes of the two components varying with wavelength (24, 25). This has been suggested to involve different protonation states of the RC. Since the kinetics become closer to exponential at low temperature, these workers have suggested that the RC may freeze preferentially into one form. In *Rb. sphaeroides*, on the other hand, the opposite findings have been reported: nonexponential (4, 26, 30) and/or wavelength-dependent (26) $P^+Q_A^-$ charge recombination kinetics at 77 K but exponential kinetics at 295 K. This has led to the proposal that the RC is trapped at low temperature in two conformations (26, 30) or a distribution of conformations (4). The same conclusion has been reached from studies on RCs with prereduced BPh_L (27) and from extensive low-temperature optically detected magnetic resonance studies (18, 28). A common postulate from these works (except ref. 25) is that at room temperature the conformers interconvert rapidly compared to the millisecond timescale of the measurements. The idea that RC conformers are individually trapped at low temperature is similar to the proposed low-temperature trapping of hemoglobin into substates having differing CO recombination kinetics (15).

Our results address similar issues, but on the subnanosecond timescale of the primary photochemical reactions. Our findings indicate that a distribution (or, again, perhaps just a few conformers) of RCs exists at room temperature and that the conformers do not interconvert on the timescale of charge separation. Each member of this population is able to carry out primary photochemistry, but with slightly different rates of electron transfer. Furthermore, our results suggest that for the most part the substates are not individually trapped at low temperature. Rather, cooling appears to shift the population into a single form (or a much smaller distribution of forms) having the fastest electron-transfer rates. Again, this may involve a general contraction of the protein. It thus appears that the RC is tolerant of some variation in both distances between the cofactors (electronic factors) and the relationship between the free-energy change and reorganization energy (the Franck–Condon factors). Such tolerance would seem to be a more practical evolutionary strategy rather than requiring the protein complex to assume a rigorously constrained architectural and energetic arrangement to carry out its function with high efficiency.

We thank Drs. D. Bocian, S. Boxer, R. Friesner, J. Rodriguez, and R. Yaris for helpful discussions. This work was supported by National Science Foundation Grant DMB-8903924.

1. Deisenhofer, J., Epp, O., Miki, K., Huber, R. & Michel, H. (1985) *Nature (London)* **318**, 618–624.
2. Allen, J. P., Feher, G., Yeates, T. O., Rees, D. C., Deisenhofer, J., Michel, H. & Huber, R. (1986) *Proc. Natl. Acad. Sci. USA* **83**, 8589–8593.
3. Chang, C. H., Tiede, D., Tang, J., Smith, U., Norris, J. & Schiffer, M. (1986) *FEBS Lett.* **205**, 82–86.
4. Kleinfeld, D., Okamura, M. Y. & Feher, G. (1984) *Biochemistry* **23**, 5780–5786.
5. Kirmaier, C., Holten, D. & Parson, W. W. (1985) *Biochim. Biophys. Acta* **810**, 33–48.
6. Woodbury, N. W., Becker, M., Middendorf, D. & Parson, W. W. (1985) *Biochemistry* **24**, 7516–7521.
7. Fleming, G. R., Martin, J.-L. & Breton, J. (1988) *Nature (London)* **33**, 190–192.
8. Gunner, M. R. & Dutton, P. L. (1989) *J. Am. Chem. Soc.* **111**, 3400–3412.
9. Marcus, R. A. & Sutin, N. (1985) *Biochim. Biophys. Acta* **811**, 265–322.
10. Bixon, M. & Jortner, J. (1989) *Chem. Phys. Lett.* **159**, 17–20.
11. Martin, J.-L., Breton, J., Hoff, A. J., Migus, A. & Antonetti, A. (1986) *Proc. Natl. Acad. Sci. USA* **83**, 957–961.
12. Kirmaier, C. & Holten, D. (1988) *FEBS Lett.* **239**, 211–218.
13. Holzapfel, W., Finkele, U., Kaiser, W., Oesterhelt, D., Scheer, H., Stilz, H. U. & Zinth, W. (1989) *Chem. Phys. Lett.* **160**, 1–7.
14. Lockhart, D. J., Goldstein, R. F. & Boxer, S. G. (1988) *J. Phys. Chem.* **89**, 1408–1415.
15. Austin, R. H., Beeson, K. W., Eisenstein, L., Frauenfelder, H. & Gunsalus, I. C. (1975) *Biochemistry* **14**, 5355–5373.
16. Kirmaier, C. & Holten, D. (1988) in *The Photosynthetic Bacterial Reaction Center-Structure and Dynamics*, eds. Breton, J. & Vermeglio, A. (Plenum, New York), pp. 219–228.
17. Won, Y. & Friesner, R. A. (1988) *Israel J. Chem.* **28**, 67–72.
18. Lous, E. J. & Hoff, A. J. (1989) *Biochim. Biophys. Acta* **974**, 88–103.
19. Bylina, E. J., Kirmaier, C., McDowell, L., Holten, D. & Youvan, D. C. (1988) *Nature (London)* **336**, 182–184.
20. Michel-Beyerle, M. E., Plato, M., Deisenhofer, J., Michel, H., Bixon, M. & Jortner, J. (1988) *Biochim. Biophys. Acta* **932**, 52–70.
21. Kirmaier, C., Blankenship, R. E. & Holten, D. (1986) *Biochim. Biophys. Acta* **850**, 275–285.
22. Becker, M., Middendorf, D., Woodbury, N. W., Parson, W. W. & Blakenship, R. E. (1986) in *Ultrafast Phenomenon V*, eds. Fleming, G. R. & Siegman, A. E. (Springer, Berlin), pp. 374–378.
23. Frauenfelder, H., Hartmann, H., Karplus, M., Kuntz, I. D., Jr., Kuriyan, J., Parak, F., Petsko, G. A., Ringe, D., Tilton, R. F., Jr., Connolly, M. L. & Nelson, M. (1987) *Biochemistry* **26**, 254–261.
24. Sebban, P. & Wraight, C. (1989) *Biochim. Biophys. Acta* **974**, 54–65.
25. Baciou, L., Rivas, E. & Sebban, P. (1990) *Biochemistry*, in press.
26. Parot, P., Thiery, J. & Vermeglio, A. (1987) *Biochim. Biophys. Acta* **893**, 534–543.
27. Tiede, D. M., Kellog, E. & Breton, J. (1987) *Biochim. Biophys. Acta* **892**, 294–302.
28. Dijkman, J. A., Den Blanken, H. J. & Hoff, A. J. (1989) *Israel J. Chem.* **28**, 141–148.
29. Peloquin, J. M., Violette, C. A., Frank, H. A. & Bocian, D. F. (1990) *Biochemistry*, in press.
30. Franzen, S., Goldstein, R. A. & Boxer, S. G. (1990) *J. Phys. Chem.*, in press.